A&A manuscript no.
(will be inserted by hand later)

Your thesaurus codes are:
05(08.16.4; 08.13.2; 10.03.1; 10.19.2; 13.09.6)

ASTRONOMY AND ASTROPHYSICS
July 6, 1999

ISOGAL-DENIS detection of red giants with weak mass loss in the Galactic Bulge *,**,***

A. Omont[1], S. Ganesh[1,2], C. Alard[3,1], J.A.D.L. Blommaert[4], B. Caillaud[1], E. Copet[5], P. Fouqué[6], G. Gilmore[7], D. Ojha[8,1], M. Schultheis[1], G. Simon[3], X. Bertou[1], J. Borsenberger[1], N. Epchtein[9], I. Glass[10], F. Guglielmo[1], M.A.T. Groenewegen[11], H.J. Habing[12], S. Kimeswenger[13], M. Morris[14,1], S.D. Price[15], A. Robin[16], M. Unavane[7], and R. Wyse[17]

[1] Institut d'Astrophysique de Paris, CNRS, 98bis Bd Arago, F-75014 Paris
[2] Physical Research Laboratory, Navarangpura, Ahmedabad 380009, India
[3] DASGAL, Observatoire de Paris, France
[4] ISO Data Centre, ESA, Villafranca, Spain
[5] DESPA, Observatoire de Paris, France
[6] ESO, Santiago, Chile
[7] Institute of Astronomy, Cambridge, U.K.
[8] T.I.F.R., Mumbai, India
[9] O.C.A., Nice, France
[10] SAAO, South Africa
[11] MPA, Garching, Germany
[12] Leiden Observatory, Leiden, The Netherlands
[13] Innsbruck, Austria
[14] UCLA, Los Angeles, CA, USA
[15] Air Force Research Laboratory. Hanscom AFB, MA, USA
[16] Observatoire de Besancon, France
[17] The Johns Hopkins University, Baltimore MD, USA

Received February; accepted May, 1999

Abstract. The ISOGAL project is a survey of the stellar populations, structure, and recent star formation history of the inner disk and bulge of the Galaxy. ISOGAL combines 15 μm and 7 μm ISOCAM observations with DENIS IJK$_s$ data to determine the nature of a source and the interstellar extinction. In this paper we report an ISOGAL study of a small field in the inner Galactic Bulge ($\ell = 0.0°$, $b = 1.0°$, area = 0.035 deg^2) as a prototype of the larger area ISOGAL survey of the inner Galaxy. The ISOCAM data are two orders of magnitude more sensitive than IRAS ones, and its spatial resolution is better by one order of magnitude, allowing nearly complete and reliable point-source detection down to ~ 10 mJy with the LW3 filter (12-18 μm) and ~ 15 mJy with the LW2 filter (5.5-8 μm). More than 90% of the ISOCAM sources are matched with a near-infrared source of the DENIS survey. The five wavelengths of ISOGAL+DENIS, together with the relatively low and constant extinction in front of this specific field, allow reliable determination of the nature of the sources.

While most sources detected only with the deeper 7 μm observation are probably RGB stars, the primary scientific result of this paper is evidence that the most numerous class of ISOGAL 15 μm sources are Red Giants in the Galactic bulge and central disk, with luminosities just above or close to the RGB tip and weak mass-loss rates. They form loose sequences in the magnitude-colour diagrams [15]/K_s-[15] and [15]/[7]-[15]. Their large excesses at 15 μm with respect to 2 μm and 7 μm is due to circumstellar dust produced by mass-loss at low rate ($\dot{M}_{dust} \sim 10^{-11}$–a few $10^{-10} M_\odot$/yr). These ISOGAL results are the first systematic evidence and study of dust emission at this early stage (Intermediate AGB and possibly RGB-Tip), before the onset of the large mass-loss phase ($\dot{M} \geq 10^{-7} M_\odot$/yr). It is thus well established that efficient dust formation is already associated with such low mass-loss rates during this early phase.

About twenty more luminous stars are also detected with larger excess at 7 and 15 μm. Repeated ISOGAL observations suggest that the majority of these are long pe-

Send offprint requests to: A. Omont, omont@iap.fr

* This is paper no. 4 in a refereed journal based on data from the ISOGAL project

** Based on observations with ISO, an ESA project with instruments funded by ESA Member States (especially the PI countries: France, Germany, the Netherlands and the United Kingdom) and with the participation of ISAS and NASA

*** Partly based on observations collected at the European Southern Observatory, La Silla Chile

riod variables with large amplitude, probably in the large mass-loss stage with $\dot{M} \geq 10^{-7} M_{\odot}$/yr.

Key words: stars: AGB and post-AGB - stars: circumstellar matter - stars: mass- loss - dust - infrared: stars - Galaxy: bulge

1. Introduction

The ISOGAL project is a multi-wavelength survey at high spatial resolution of the inner Galaxy. The general scientific aims are to quantify the spatial distributions of the various stellar populations in the inner Galaxy, together with the distribution of the warm interstellar medium (ISM). Optical, near-IR and mid-IR (to 15 μm) data with near arcsec spatial resolution are being obtained covering the central Galactic bulge, and sampling the obscured disk within the Solar circle. Complementary data at other wavelengths are being obtained in regions of specific interest. To date, most ISOGAL effort has focussed on a large area broad-band imaging survey at 7 μm and 15 μm with ISOCAM on the ISO satellite, and on complementary DENIS IJK$_s$ observations of the central Galaxy. A full description of the ISOGAL project will be published elsewhere (Omont et al, in preparation). First imaging results are available (Pérault et al 1996), as is a complementary paper to this, discussing late type giants at somewhat higher Galactic latitudes (Glass et al 1999). In this paper we discuss first results on the luminous AGB stellar population in the previously unobserved inner bulge (see also Frogel et al 1999), from observations of a field whose line of sight projects some 140pc above the Galactic centre, on the minor axis.

The AGB stage is one of the most complex phases of stellar evolution, while at the same time being of crucial importance for nucleosynthesis and galactic chemical evolution. Although it is clear that mass-loss dominates the final evolution of AGB stars, the detailed physics of this process remains rather uncertain. Theoretical progress in the past years has emphasized the relationship between mass-loss and luminosity and hence thermal pulses, radiation pressure on dust and stellar pulsations of long period variables (LPV). The status of recent modelling and the observational data are fully reviewed by Habing (1996) [see also the proceedings of IAU Symposium 191 edited by Le Bertre et al. (1999)]. Observationally, rates of mass loss are relatively well documented, especially from millimeter CO studies, far infrared IRAS results and near infrared studies. However, this direct knowledge of AGB mass-loss is mostly limited to the solar neigbourhood. In particular, in the galactic bulge and central disk, IRAS was able to detect only the relatively few AGB stars with the largest mass-loss rates $\geq 10^{-6}$ M$_{\odot}$/yr. We are indeed still lacking the observational information to characterize the influence of metallicity and initial mass on the properties of mass-loss on the AGB. Near infrared observations, and in particular the DENIS (Epchtein et al. 1997) and 2MASS (Skrutskie et al. 1997, Cutri 1998) surveys, can detect practically all the AGB stars in the Galaxy. However, it is extremely difficult to both identify an AGB star, and to distinguish between small to moderate mass-loss rates and patchy interstellar extinction, solely from near-infrared data in regions of high extinction. Data at longer wavelengths, which are more sensitive to the infrared excess that is a consequence of mass loss, and less sensitive to interstellar reddening, are required. Mid-infrared post-IRAS space surveys, such as the present surveys with ISOCAM and MSX (Price et al. 1997, Egan et al. 1998) are thus uniquely suited for carrying out a census of mass-losing AGB stars in the inner Galaxy and for quantifying the distribution function of mass loss-rates.

Our ISOGAL survey of selected regions of the inner Galaxy, at 15 and 7 μm (Pérault et al. 1996, Omont et al. 1999a,1999b) has a sensitivity two orders of magnitude better than IRAS, and their spatial resolution is better by one order of magnitude. The main purpose of this paper is to show that the ISOGAL data, which combine ISOCAM mid-infrared observations with near-infrared DENIS data, are ideal to identify bulge mass-losing AGB stars, even with dust mass-loss rates as small as 10^{-11} M$_{\odot}$/yr.

We analyse here the ISOGAL/DENIS data of a small field (area 0.035 deg^2) centered at $\ell = 0.0°$, $b = 1.0°$ in the inner bulge. This field is approximately one-half a bulge scale height down the minor axis, in a previously poorly studied region mid-way (in $|b|$) between the innermost optical "windows" (Glass et al. 1999) and the Galactic centre.

The very high stellar density in this field leads to a near confusion-limited survey, thus providing a maximum number of detected sources, the majority of them in the bulge and central disk. The relatively low and well behaved extinction allows reliable identification of mass-losing AGB stars down to the RGB tip (K$_0$ $\sim$ 8.2 for D = 8.0 kpc, Tiede et al 1996). It permits also easier comparisons with earlier works on (apparently fainter) stars of the red giant branch (RGB), LPVs and IRAS sources in the more outer bulge (see e.g. Frogel & Whitford 1987, Frogel et al. 1990, Tiede et al. 1996, Glass et al. 1995, van der Veen & Habing 1990 and references therein). We can also compare the data with those of the companion paper (Glass et al. 1999) on ISOGAL observations in two fields of the Baade Windows. The analysis of the stellar sources is made easier in the latter by the smaller extinction, the greater distance from the galactic disk and previous identifications of LPVs from optical surveys.

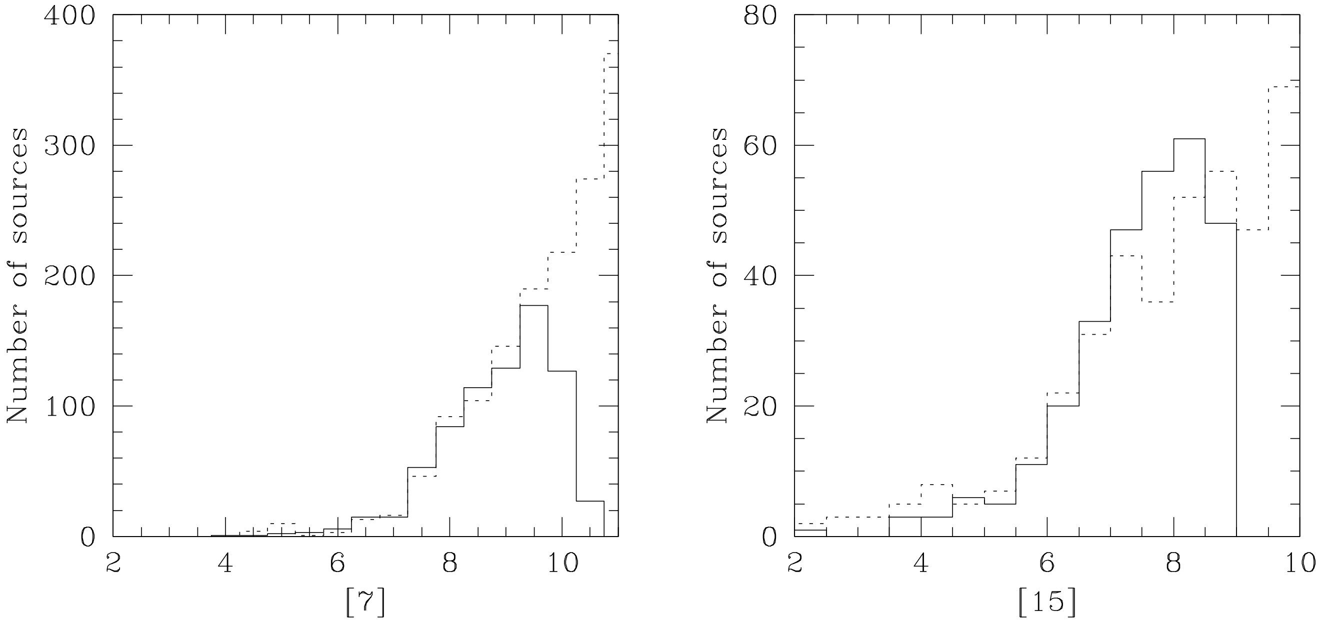

Fig. 1. LW2 and LW3 source distributions in half magnitude bins. Solid lines indicate the number of detected sources. Dotted lines indicate the approximate expected number of sources based on $LW2_{exp}$ = ([5 × K_s] - 10.5) / 4.0 and $LW3_{exp}$ = ([1.84 × LW2] - 8.5) / 0.84 for detections in K_s and LW2 respectively (see Appendix B.4).

Table 1. Journal of ISOCAM and DENIS observations in the $\ell = 0.0°$, $b = 1.0°$ field

Identification	Filter	Pixel Size	Julian Date	Remarks
13600327$^{(b)}$	LW3	6″	2450174	12-18 μm
32500256$^{(b)}$	LW2	6″	2450363	5.5-8.5 μm
83600417$^{(a)}$	LW2	3″	2450873	
83600418$^{(b)}$	LW2	6″	2450873	
83600522$^{(a)}$	LW3	3″	2450873	
83600523$^{(b)}$	LW3	6″	2450873	
DENIS 96$^{(a)}$	I,J,K_s	1″,3″,3″	2450184	
DENIS 98$^{(b)}$	I,J,K_s	1″,3″,3″	2450951	

Notes.$^{(a)}$ Data used in the present paper.
$^{(b)}$ These observations have only recently become available and are not fully used in the present paper.

2. Observations; Data Reduction and Quality; Cross-Identifications.

2.1. ISOGAL Observations

This field, $\ell = 0.0°$, $b = 1.0°$, is one of the fields used to quantify the reliability of ISOGAL data. We have thus at our disposal repeated observations at different dates as detailed in Table 1. This allows us to check reliability of detected sources, and additionally to identify (long period) variables. Our usual ISOGAL ISOCAM data use 6″ pixels. Here we also have observations with 3″ pixels (7 & 15 μm), allowing deeper photometry since confusion rather than photon noise limits the detections. A detailed evaluation will be presented elsewhere in a general assessment of the quality of the ISOGAL data. We will summarise here a few conclusions relevant for the present state of data reduction and the scientific case of this paper.

The 3″ ISOCAM [1] observations mainly used in this paper were performed in revolution 836 (28 February 1998) at 15 μm (filter LW3, 12-18 μm) and at 7 μm (filter LW2, 5.5-8.5 μm). The two year delay with respect to the IJK_s DENIS observations should be taken into consideration for the few strongly variable stars. However, we have another 15 μm observation at a date reasonably well matched with that of the DENIS observations.

In addition to the usual problems with the ISOCAM data (glitches, dead column, time dependant behavior of the detectors), the difficulties of reduction of the ISOGAL data are more severe for several reasons: crowding of the fields which is often close to the confusion limit, highly structured diffuse emission, high density of bright sources which induce long-lasting pixel-memory effects, integration times per raster position short compared to detector stabilisation times, etc. Therefore, a special reduction pipeline was devised (Alard et al. in preparation) which is more sophisticated than the standard treatment applied to the ISOCAM data. A detailed discussion of data quality is given in Appendix B.

[1] see Cesarsky et al. 1996 for a general reference to ISOCAM operation and performances

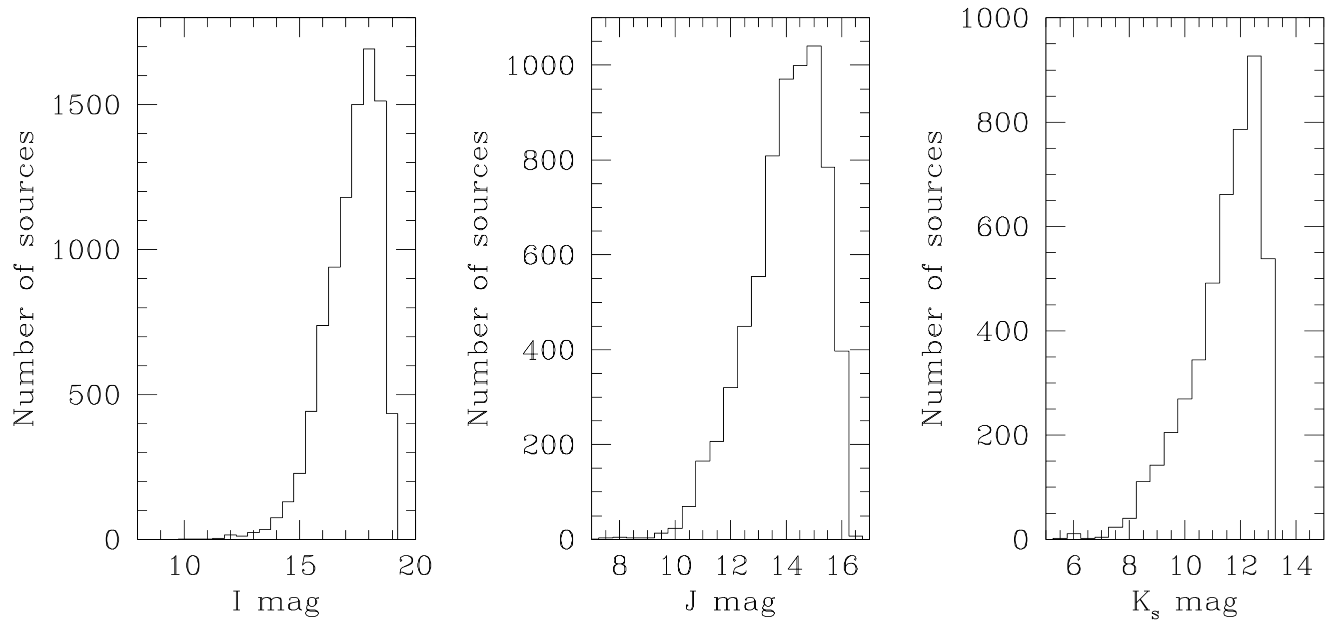

Fig. 2. DENIS source counts in I, J, K_s bands in half magnitude bins

The histograms of the 7 and 15 μm source counts derived from the 3″ ISOGAL observations are displayed in Figure 1. In order to ensure a reasonable level of reliability, completeness and photometric accuracy, we presently limit the discussion of ISOGAL data to sources brighter than 8.5 mag (8 mJy) for LW3 sources and 9.75 mag (11 mJy) for LW2 sources (the fluxes and magnitudes used are defined in Appendix A). The source counts in this field are thus 599 and 282 respectively in LW2 and LW3.

The source density is relatively close to the confusion limit for LW2 sources (85 pixels [3″ × 3″] per source). However, the LW3 observations are farther from confusion since their density is twice smaller than for LW2 sources.

2.2. DENIS Observations

The near infrared data were acquired in the framework of the DENIS survey, in a dedicated observation of a large bulge field (Simon et al. in preparation), simultaneously in the three usual DENIS bands, K_s (2.15 μm), J (1.25 μm) and Gunn-I (0.8 μm). Following the general reduction procedures for DENIS data (Borsenberger et al. in preparation), and after the preliminary analysis of the same data by Unavane et al. (1998), we optimised the source extraction for crowded fields (Alard et al. in preparation). Since for the majority of the ISOGAL sources in this particular field (giants with little dust and small reddening), the DENIS sensitivity is much better than that of ISOGAL (by typically 3 magnitudes), consideration of the faintest DENIS sources is not critical for our purposes. The histograms of the DENIS K_s, J, I sources are shown in Figure 2. The quality of this DENIS data is briefly discussed in Appendix B. The sensitivity is mostly limited by confusion in the K_s and J bands. The completeness limit is thus probably close to 11.5 in the K_s band and 13.5 in the J band (i.e. about two magnitudes lower than in "normal" uncrowded DENIS fields).

One problem with the DENIS data is the saturation of the detectors for very bright sources. We thus presently do not use the DENIS data for the 12 sources with K_s < 7, not only for the K_s band, but also for the I and J bands where the signal is saturated as well. For slightly fainter sources the corrections for saturation are not yet optimised and the DENIS photometry will be improved in the future.

The catalog used to make the DENIS astrometry is the PMM catalog, referenced as the "USNO-A2.0" catalog. The absolute astrometry is then presently fixed by the accuracy of this catalog (namely 2″, with an rms of 1″). The internal accuracy of DENIS observations, derived from the identifications in the overlaps, is of the order of 0.5″. This excellent astrometry is of course used to improve that of ISOGAL sources. The DENIS data are also extremely useful to derive the interstellar extinction toward ISOGAL sources (see Section 3).

2.3. Cross-identification of ISO and DENIS sources

Cross-identifications of LW3 and LW2 sources, between themselves and with DENIS sources, provide the multicolour data which allow discussion of the nature and properties of individual sources which makes up the bulk

Table 2. Catalog of bright ISOGAL+DENIS sources in the $\ell = 0, b = 1$ field ([7] < 7.5)

No.	Name	I	J	K_s	[7]	[15]	Cross-identifications and comments
14	ISOGAL-DENIS-P J174116.3-282957		10.75	8.00	7.23	5.86	
23	ISOGAL-DENIS-P J174117.5-282957	15.87	9.78	S	6.44	5.12	
61	ISOGAL-DENIS-P J174122.6-283148				4.17	2.30	V, IRAS17382-2830
94	ISOGAL-DENIS-P J174126.3-282538		11.32	8.41	7.13	5.93	
99	ISOGAL-DENIS-P J174126.6-282702	17.27	10.41	7.37	6.00	4.47	V
108	ISOGAL-DENIS-P J174127.3-282851	16.01	10.03	7.43	6.31	5.01	V
119	ISOGAL-DENIS-P J174127.9-282816	15.30	9.63	7.14	6.66	5.67	
124	ISOGAL-DENIS-P J174128.5-282733	15.47	9.80	7.27	6.73	5.96	V
134	ISOGAL-DENIS-P J174129.4-283113	14.78	10.19	7.98	7.33	6.68	
148	ISOGAL-DENIS-P J174130.4-283225	S	8.14	S	6.57	6.67	F
158	ISOGAL-DENIS-P J174131.2-282815	15.06	9.89	7.51	7.01	6.51	
212	ISOGAL-DENIS-P J174134.4-283349	10.22	8.01	S	6.52	6.67	F
213	ISOGAL-DENIS-P J174134.4-282922	S	S	S	4.76	3.79	
218	ISOGAL-DENIS-P J174134.6-282431	16.76	10.53	7.96	6.51	5.57	V
220	ISOGAL-DENIS-P J174134.7-282313	15.12	10.61	8.34	7.49	7.73	
252	ISOGAL-DENIS-P J174137.2-282904	15.82	10.79	8.29	7.45	6.33	
255	ISOGAL-DENIS-P J174137.4-282630	15.62	10.59	8.17	7.46	6.93	
270	ISOGAL-DENIS-P J174138.3-282447	15.37	10.35	8.11	7.46	6.74	
272	ISOGAL-DENIS-P J174138.3-282338	15.35	10.15	7.96	7.41	6.70	
275	ISOGAL-DENIS-P J174138.6-282743	16.44	10.76	8.28	7.00	6.14	
289	ISOGAL-DENIS-P J174139.1-282644		10.31	7.55	6.65	5.68	
296	ISOGAL-DENIS-P J174139.5-282428	15.49	9.67	S	5.98	4.72	V
304	ISOGAL-DENIS-P J174139.9-282520	15.21	9.69	7.31	6.68	4.80	
310	ISOGAL-DENIS-P J174140.1-282220	11.99	9.02	7.31	7.22	7.30	F
334	ISOGAL-DENIS-P J174141.5-282540	16.46	10.44	8.00	7.28	6.17	
335	ISOGAL-DENIS-P J174141.5-281930	14.36	9.74	7.60	7.06	7.11	F
349	ISOGAL-DENIS-P J174142.1-283049	15.68	11.01	8.55	7.34	6.71	
362	ISOGAL-DENIS-P J174142.6-282641	17.59	11.11	8.18	6.61	5.21	V
363	ISOGAL-DENIS-P J174142.7-283116		11.62	8.61	6.62	5.26	
391	ISOGAL-DENIS-P J174144.5-282034		10.15	8.04	7.15	6.21	
414	ISOGAL-DENIS-P J174145.4-282824	15.28	10.44	8.15	7.41	6.40	
433	ISOGAL-P J174146.5-282259				5.08	3.83	
442	ISOGAL-DENIS-P J174147.3-282506	16.21	10.46	8.15	7.33	6.29	
511	ISOGAL-DENIS-P J174151.4-281739	16.38	10.13	7.47	7.00	6.07	
522	ISOGAL-DENIS-P J174151.8-282455	S	S	S	4.72	4.88	F, V
529	ISOGAL-DENIS-P J174152.1-281839	16.72	10.57	8.07	7.44	6.65	
533	ISOGAL-DENIS-P J174152.2-281601	13.58	10.00	7.76	6.63	6.33	V
537	ISOGAL-DENIS-P J174152.6-282015	16.30	10.63	8.06	7.38	6.21	
539	ISOGAL-DENIS-P J174152.8-281720	14.79	10.05	7.74	7.20	6.72	
548	ISOGAL-DENIS-P J174153.2-282621	15.05	9.75	7.36	6.85	6.04	
550	ISOGAL-DENIS-P J174153.3-282535	13.76	9.80	7.69	7.34	7.31	F
552	ISOGAL-DENIS-P J174153.4-282027	13.95	9.75	7.68	7.30	7.31	F
559	ISOGAL-DENIS-P J174153.8-282739	17.23	11.24	8.63	7.30		
576	ISOGAL-DENIS-P J174154.6-282133	16.20	10.54	8.29	7.45	6.29	
579	ISOGAL-DENIS-P J174154.7-282659	15.05	9.26	S	5.75	4.47	V
581	ISOGAL-DENIS-P J174154.8-281731	16.40	9.98	7.32	6.37	5.39	V
595	ISOGAL-DENIS-P J174155.3-281638	15.66	9.59	S	5.99	4.49	
606	ISOGAL-DENIS-P J174155.9-282358	14.12	10.09	8.05	7.44	6.85	
642	ISOGAL-DENIS-P J174157.5-282237	15.39	9.91	7.60	6.94	5.86	
660	ISOGAL-DENIS-P J174158.7-281849		10.13	7.41	5.92	4.52	
668	ISOGAL-DENIS-P J174159.3-282554	11.60	8.86	S	6.99	6.79	V
674	ISOGAL-DENIS-P J174159.8-281901	16.80	10.71	8.17	7.49	6.45	
682	ISOGAL-DENIS-P J174200.3-282303	12.20	8.16	S	5.67	4.93	F?, V
701	ISOGAL-DENIS-P J174201.9-281802	16.76	10.58	8.01	7.37	6.35	
716	ISOGAL-DENIS-P J174202.8-282124	16.16	10.39	8.10	6.41	5.75	V, Terzan V 3126
723	ISOGAL-DENIS-P J174203.2-282107	12.09	8.36	S	6.43	6.32	F
725	ISOGAL-DENIS-P J174203.7-281729	16.98	10.52	7.61	5.89	4.58	V
732	ISOGAL-DENIS-P J174204.3-282137	13.52	9.33	7.33	6.79	6.92	F
753	ISOGAL-DENIS-P J174206.8-281832	17.59	10.68	7.65	5.49	3.87	V
791	ISOGAL-DENIS-P J174213.8-281827	12.85	8.65	S	6.11	5.63	F
794	ISOGAL-DENIS-P J174215.1-281850	16.34	10.37	7.78	6.86	5.85	
799	ISOGAL-DENIS-P J174216.3-281947	15.49	10.34	8.05	7.18	6.71	

Note. F = Foreground or suspected foreground star, V = Variable or suspected variable star, S = Saturated source of this paper (Figures 3 to 9 discussed below). The cross-identification process is also useful for determining data quality. We have now routine standard procedures for ISOGAL-ISOGAL and DENIS-ISOGAL cross-identifications (see Appendix B). A substantial fraction of the ISO sources have thus been identified with DENIS sources (93% and 84% for LW2 and LW3 sources respectively).

Cross-identifications are essential to establish the reliability of the ISOGAL detections. Indeed, because of possible residual artifacts, mainly due to pixel memory or of noise peaks simulating sources, we consider that the reality of a weak ISOGAL source is not yet well warranted here if it is not confirmed by another detection, either in the other ISOGAL band, or in the K_s band. Only 9% of LW3 sources are not associated with an LW2 or a K_s source. The proportion of unassociated LW2 sources is slightly smaller, 5%.

In order to check the completeness of LW3 sources, we can use the more sensitive LW2 observations; DENIS K_s detections can be used in a similar way to estimate the completeness of LW2 sources (see Appendix B and Figure 1). The completeness is probably close to 80% at least, for [7] $<$ 9.5 and for [15] $<$ 8.5. A more detailed analysis of the source surface density, and its implications for the structure of the Galactic bulge, will appear elsewhere, following more sophisticated modelling of source incompleteness as a function of position in this and other fields. For present purposes such an incompleteness is not a limiting factor.

The quality of ISOGAL photometry has been checked in this field and others by repeated observations (see Appendix B and Ganesh et al. in preparation). The uncertainty thus proved to be better than ~ 0.2 mag rms above $\sim$ 15 mJy in both bands. However, there is not yet a good standard procedure to fully correct for the detector time behaviour effects for fields such as ISOGAL ones with strong sources and background. Because of that and of confusion, our photometry is thus still uncertain by a few tenths of a magnitude systematically.

In conclusion, we consider the reliability of the existence of most of the sources discussed to be well established. The completeness is also well characterised. However, the photometric accuracy can still be improved.

Table 2 gives a catalogue of bright ISOGAL sources ([7] $<$ 7.5), with three-band DENIS associations and identification of foreground sources and of candidate variable stars. A complete catalogue of all ISOGAL sources will be available at CDS by October 1999, when the data reduction is improved.

3. Near infrared data and interstellar extinction

The data at five wavelengths available for most of the sources allow in most cases a good characterisation of the ISOGAL sources, with some redundancy, as well as of their

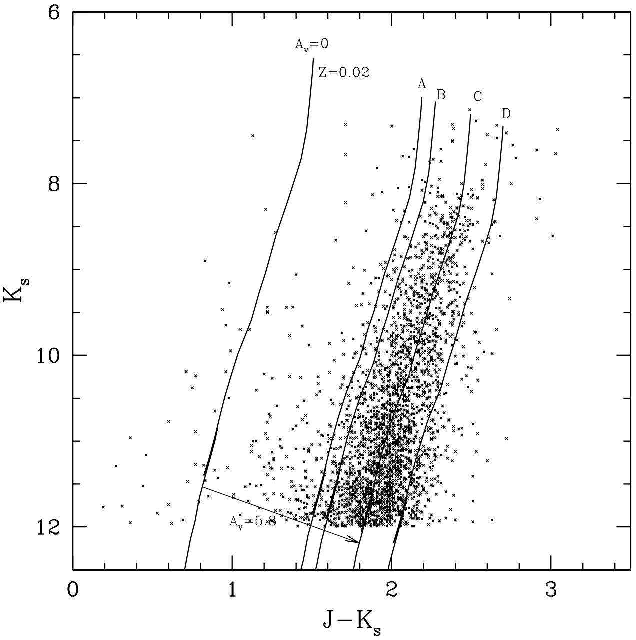

Fig. 3. Colour magnitude diagram (J-K_s) / K_s for all unsaturated DENIS sources in the field. An isochrone (Bertelli et al. 1994), placed at 8 kpc distance, is shown for a 10 Gyr population with Z=0.02. The near-infrared colours of this isochrone have been computed with an empirical $T_{\rm eff} - (J-K)_0$ colour relation built by making a fit through measurments see Ng et al (in preparation) for details about this relation. The labels A,B,C,D identify the isochrones shifted by A_V of 4, 4.5, 5.8 and 7 respectively.

interstellar reddening. The very large stellar density in the inner bulge and central disk brings a considerable simplification by ensuring that the majority of the sources are located within it. In addition, it happens that the interstellar extinction is relatively small on this line of sight and nearly constant for this whole small field. The discussion of the nature of the sources and of their properties, such as mass-loss, is thus much easier.

The multi-dimensional analysis of magnitude-colour space defined by these data allows one to visualise and to determine the source properties. Deferring detailed discussions to the next sections, we limit this section to a general presentation of these diagrams and of the general information they provide about interstellar extinction, circumstellar dust emission and circumstellar absorption.

The K_s/J-K_s magnitude-colour diagram of all DENIS sources in our field (Figure 3) shows a remarkably well-defined bulge red giant sequence shifted by fairly uniform extinction of A_V=5.8±1 mag. with respect to the reference $K_{s\,o}$ *vs* $(J-K_s)_o$ of Bertelli et al. (1994) [2] with Z = 0.02

[2] The isochrones by Bertelli et al. have been computed in the ESO system using the ESO filter curves. From NIR spectra for a sample of oxygen-rich M stars and carbon stars, K-K_s values have been computed. The differences are very small (on average

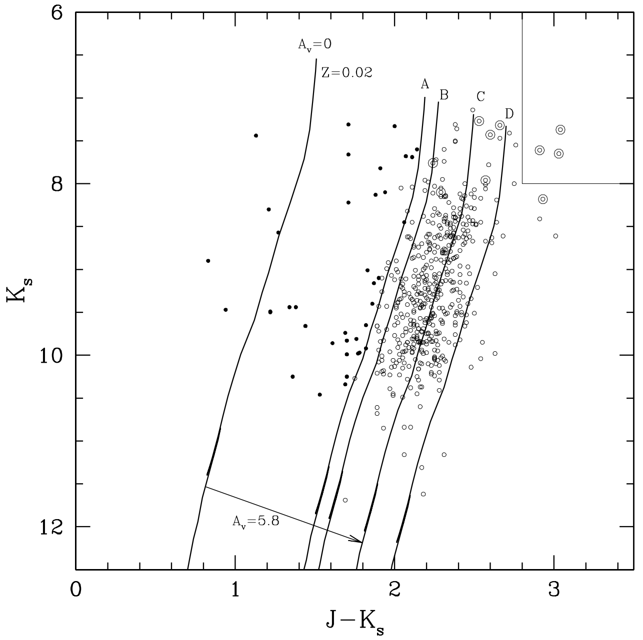

Fig. 4. Colour magnitude diagram (J-K$_s$)/K$_s$ for unsaturated DENIS sources with [7] or [15] counterparts in the field. Filled circles represent the foreground sources with consistent data in the other diagrams. Suspected variables (see text and Section 6) are indicated additionally by large open circles. The labels A,B,C,D and isochrones are as described in Figure 3. The region where J-K$_s$ is indicative of high mass-loss AGB (see Section 6) is delimited by the boxed region to upper right.

and a distance modulus of 14.5 (distance to Galactic Centre 8 kpc; we have assumed that $[A_J\text{-}A_{K_s}]/A_V = 0.167$). Most of the extinction should thus be associated with interstellar matter outside of the bulge. We have checked from the individual values of A$_V$ and the DENIS source counts that there is apparently no strong spatial variation of the extinction in this field. The ISOGAL sources with anomalously low values of A$_V$ are probably foreground. They are visible in Figure 4, which shows the subset of the K$_s$/J-K$_s$ sources of Figure 3 which were also detected at longer wavelengths. There is of course some uncertainty for the marginal cases: for bright sources with good photometry (K$_s$ < 10), those located left of line A ($A_v < 4$) are almost certainly foreground, while those to the right of line B ($A_v > 4.5$) are very probably in the "bulge", and the case is uncertain for those between lines A and B. The case of foreground ISOGAL sources will be further discussed below. Those with $A_v < 4$ and with consistent data in the other diagrams are identified by special symbols in the various diagrams.

about 0.04 mag for the M giants), so concerning the internal dispersion in K we can neglect it. This result is in agreement with Persson et al. (1998) who presented a new grid of infrared standard stars in J, H, K and K$_s$.

The distribution of sources about line C is dominated by photometric errors, and residual extinction variations. There is no evidence for a significant background population, more highly reddened, in the disk beyond the Galactic centre, though a few such sources may be present. Similarly, it is difficult from just these data to identify any intrinsic red J-K$_s$ excess in sources below the RGB-tip, which is near $K_{s,0} = 8.2$ (Tiede et al 1996). The J-K$_s$ excess of the six bright sources much redder than line D is very probably related to an intrinsic J-K$_s$ excess generated by a relatively thick dusty circumstellar shell, as confirmed by the very large value of K$_s$-[15] for these sources (see Section 6). A few other sources, just redder than line D in Figure 4, might also have an intrinsic J-K$_s$ excess. Only in the situation of relatively small, foreground, and uniform interstellar extinction, could even a fraction of the AGB stars with high mass-loss be identified, and their mass-loss characterised, from the near-infrared DENIS (or 2MASS) data alone. In general, longer wavelength data are critical.

The I band data, when they exist, can provide additional interesting constraints. However, the much larger spread of intrinsic I-J values in the bulk of the distribution, compared to J-K$_s$ complicates the identification of foreground sources from I-J data alone. While (J-K$_s$)$_\circ$ is confined to a very small range (∼ 0.5 mag) for most sources, it is well known (see, e.g., Frogel & Whitford 1987, Appendix A) that there is a large spread in the I magnitudes of bulge AGB giants and hence in (I-J)$_\circ$, that we find ranging over more than 2 magnitudes. Such a spread is certainly related to the behaviour of the TiO absorption bands, and hence probably to the metallicity. However, there is as yet no very detailed modelling of this behaviour.

The average value of I-J increases by about 1.5 mag. along the intermediate-AGB sequence defined in Section 5.

4. The Nature of the ISOGAL Sources

As discussed below, the most numerous classes of sources detected both at 7 & 15 μm in the ISOGAL survey are probably "bulge" intermediate AGB stars or RGB tip stars with low mass-loss, and high mass-loss rate AGB stars ($\dot{M} \geq 10^{-7} M_{\odot}$/yr). These are discussed in detail below. In this section we consider first minor populations in the survey.

There are practically no good young star candidates among ISOGAL sources in this field. They should be found among sources with large 15μm excess that are too faint to be AGB stars with large mass-loss. There are no really convincing cases in the diagrams of Figures 6 & 7 (however, see Section 5). This is consistent with the relatively small value of A$_v$, indicating that there is no very thick molecular cloud on the line of sight.

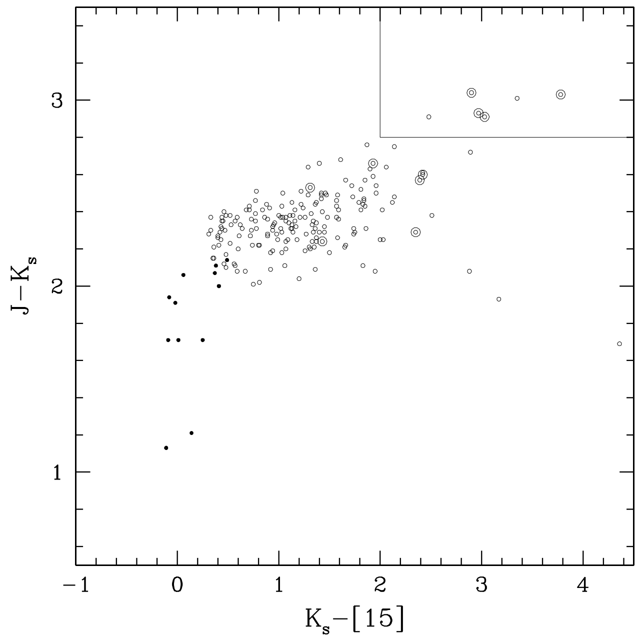

Fig. 5. J-K_s/K_s-[15] colour-colour diagram of LW3 sources with unsaturated DENIS counterparts. All symbols are as in Figure 4.

4.1. Foreground stars with little or no reddening

Some 40 stars ($\sim$ 7% of ISOGAL sources with DENIS counterparts) which lie to the left of line A (A_V~4) in Figure 4 are probably foreground stars, in front of the main line of sight extinction. This is independently confirmed by another colour for most of them. The brightest 19 stars, with $K_s \lesssim 9$, are detected in LW3 with colours $0.1 < K_s$-$[15] < 0.5$ and apparent magnitudes consistent with their being foreground disk giants. The fainter sources are consistent with being either M giants with very low reddening, or moderately reddened disk K giants.

One should add to these probable foreground stars, a few very bright sources saturated in the DENIS data. Seven such stars are thus tentatively identified in the ISO data. Let us stress that the identification of foreground stars is more difficult for bright sources (K $\lesssim$ 8) because the intrinsic colour (J-K_s)$_0$ is more uncertain. Altogether, we have thus identified about 8% of the ISOGAL sources as foreground stars. They are distinguished by special symbols in Figures 4 to 9.

4.2. 7μm sources without 15μm detections

As described above, the ISOGAL sensitivity is much greater in the LW2 band than in the LW3 band for red giants with no or little dust. The number of sources detected in LW2 is more than twice that in LW3. Most sources detected with LW2 and not with LW3 are fainter in the LW2 and K_s bands than are the detected LW3 sources (see Figure 9).

We are able to define the nature of these sources reliably, since the interstellar extinction is well characterised on this line of sight. Few, if any, of the sources detected only at 7 μm can have intrinsic infrared excess, from circumstellar dust, or they would have been readily detected at 15 μm. The foreground sources are identifiable from combination of the DENIS and 7 μm flux. Thus, one may isolate those sources which are predominately bulge RGB sources, below the RGB tip (see Figure 9). An analysis of the bulge density distribution of both AGB and RGB stars, based on their surface density distribution, will be provided elsewhere. This analysis however requires very careful modelling, as the faint source counts are strongly affected by incompleteness (see e.g. Unavane et al 1998).

5. Mid-Infrared Data and Intermediate AGB stars

The main additional information in the ISO mid-infrared bands with respect to the shorter wavelength data solely from DENIS, is the much increased sensitivity to emission from cold circumstellar dust. This is well exemplified by the J-K_s/K_s-[15] colour-colour diagram of Figure 5. While the range of J-K_s values is restricted to ~0.5 mag for most sources (with another 0.5 mag for a few sources), K_s-[15] ranges from 0 to 2.2 for the bulk of the sources (with an extension up to 4 magnitudes for a few sources). The colours [7]-[15] and K_s-[7] (Figures 7 & 9) also display large ranges of excess, although somewhat smaller than for K_s-[15].

As we discuss now, only the presence of circumstellar dust can explain such a large excess; only a portion of it can be attributed to the very cold photosphere.

In the magnitude-colour diagrams [15]/K_s-[15] and [15]/[7]-[15] (Figures 6 & 7, respectively), the majority of the sources follow a loose linear sequence. Characteristic values of the colours and magnitudes corresponding to the two ends of this sequence are given in Table 3. The magnitude of the lower end of the sequence accidently coincides with the ISOGAL sensitivity at 15μm. It is almost exactly that of the tip of the bulge RGB ($K_{\rm o} \sim 8.2$, Tiede et al 1996, $K_{\rm o} \sim 8.0$, Frogel et al 1999) [3].

[3] The magnitude spread from the line of sight effect of the bulge is very model-dependant. Perhaps the most reliable first estimate can be derived from recent models of the COBE photometry (Binney et al. 1997), which Glass et al (1999) show are reasonably consistent with the ISOGAL source counts in the inner Galaxy. These analyses derive a bulge density profile which is approximately exponential with scale length smaller than 300pc. For an adopted galacto-centric distance of 8kpc, this introduces a width of $\sim$ 0.1mag per scale length. In their study of Sgr I Miras, Glass et al 1995 have found a dispersion sigma of 0.35 mag from the regression line in the K logP diagram. This gives an upper limit for the dispersion caused

Table 3. Values of colours and magnitudes for the base and the tip of the mass-loss AGB sequence ("intermediate-AGB sequence") in the magnitude-colour diagrams Figures 6, 7 & 8.

	K_s-[15]	[7]-[15]	[15]	K_s	$(K_s\text{-}[15])_0$	K_{s0}	M_K [a]	$M_{bol}^{(b)}$	$L(L_\odot)$
Tip	2.2	1.4	5.8	8.0	1.8	7.5	-7.0	-4.0	3200
Base	0.4	0.0	8.5	8.9	0	8.4	-6.1	-3.1	1400

Notes. [a] with a distance modulus of 14.5 (D = 8 kpc)
[b] with the K bolometric correction M_{bol} - M_{Ks} = 3.0 (Groenewegen 1997), which yields M_{bol}~K_s-12 in this field.

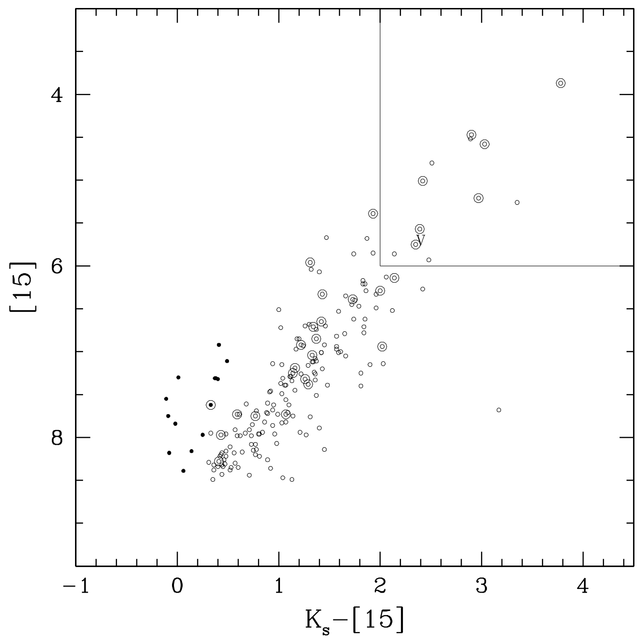

Fig. 6. [15]/K_s-[15] magnitude-colour diagram of ISOGAL sources with unsaturated DENIS counterparts. Symbols are as in Figure 4. All the possible candidate variables selected by the method described in Section 6 are indicated by large open circles. However, those with [7] ¡ 7.0 are considered as dubious and they are discarded in the other figures. The Terzan variable (see text) is refered by the symbol V in this figure. The region of high mass loss AGB is demarcated by the boxed region.

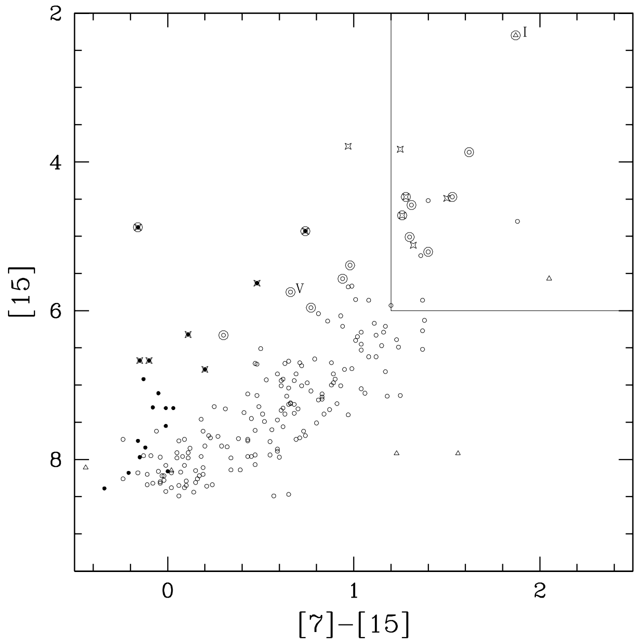

Fig. 7. [15]/[7]-[15] magnitude-colour diagram of ISOGAL sources. Sources saturated in DENIS observations are shown by filled (foreground) and open (bulk) crosses in this figure. Sources without DENIS counterparts are shown by open triangles. The Terzan variable is denoted by V and the IRAS source by I (see text). The region of high mass loss AGB is demarcated by the boxed region. All other symbols are as in Figure 4.

Since there is some uncertainty about the position of the base of the sequence with respect to the RGB tip, it is difficult to know whether the 15μm sources with the smaller infrared excess (K_s-[15] $\lesssim$ 1) are intermediate-AGB or RGB-tip stars. However , most of the sequence with larger 15 μm excess (K_s-[15] $\gtrsim$ 1) seems to correspond to AGB stars up to ~1 mag in K_s brighter than the RGB tip. This K_{s0} magnitude range, 7.5 - 8.5, corresponds to M spectral types from M6 to M9 (see Table 3A of Frogel & Whitford 1987 and Figs 10 and 12 of Glass et al. 1999). Since these stars are fainter by one or two magnitudes in $K_{s\circ}$ or M_{bol} than the few very luminous AGB stars discussed in Section 6, we propose to describe this sequence as "the intermediate-AGB mass-loss sequence".

by front-to-back spread, at least in the Sgr I region. Thus, line of sight spreads in the photometry, for fields near the minor axis where systematic bar-induced effects are unimportant, are probably small compared to other uncertainties. Of course, the magnitude spread is much larger for the minor, but non negligible, number of sources of the central disk: ~0.9 mag per 2.7 kpc scale length

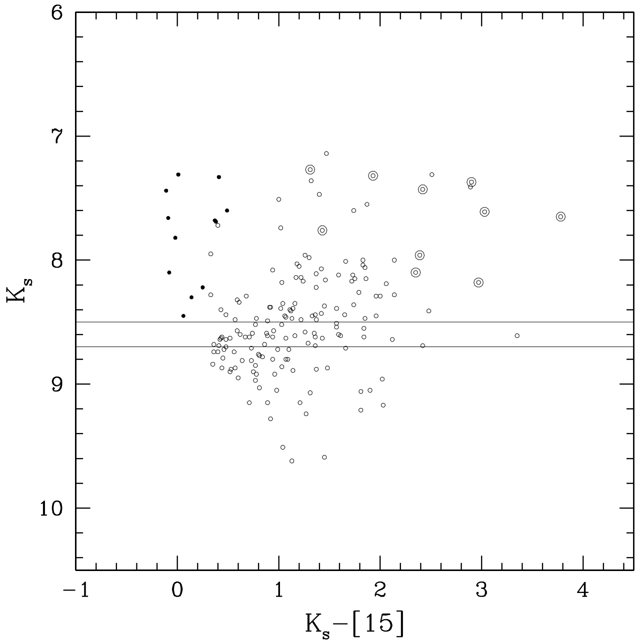

Fig. 8. K_s/K_s-[15] magnitude-colour diagram of ISOGAL sources detected both in LW2 and LW3, with unsaturated DENIS counterparts. The approximate position of the RGB tip (taking into account the interstellar extinction in this field) is shown by the solid lines at K_s=8.7 ($K_0 \sim 8.2$, Tiede et al. 1996, $A_K \sim 0.5$) and K_s=8.5 ($K_0 \sim 8.0$, Frogel et al. 1999). All symbols are as in Figure 4.

There are also some stars with large 15μm excess (K_s-[15] > 1) apparently significantly below the RGB tip (see Figure 8). However, we have checked that the majority (8 out of 13) have very poor photometry because of blends. The nature of the few remaining cases is unclear: photometry or association problems, background AGBs, young stars or red giants below the RGB tip (AGB or RGB) with mass-loss?

In order to explore the amount of circumstellar dust involved and its properties, we have used the models developed by one of us (MG) which calculate absolute magnitudes within the relevant ISOCAM and DENIS filters. The most robust conclusion from the models is confirmation of the need for circumstellar dust to achieve such large infrared excess with respect to photospheric emission. Without dust the K_s-[15] colours for giant spectral types M5, M8 and M10 are only 0.15, 0.55 and 1.07, respectively. As concerns the specific dust model, in the absence of detailed information, the simplest assumption is a time-independent dust mass-loss rate $\dot{M}_{dust}$. Of course the value of M_{dust} inferred from the DENIS-ISOGAL colours strongly depends on the assumed intrinsic dust properties. Depending on these properties, the dust mass-loss rate of the tip of the intermediate AGB sequence ranges from $\dot{M}_{dust}$ = $\sim$$10^{-10}$ $M_\odot$/yr to $\sim$5 10^{-10} $M_\odot$/yr. The infrared colours of the beginning of the intermediate AGB sequence imply mass-loss rates 10-30 times smaller than for the tip.

An appropriate value of the dust-to-gas ratio during mass loss remains an open question. The range of spectral type and of mass-loss rate discussed above is typically the domain of validity of the Reimers formula (1975) for the total mass-loss rate $\dot{M}$. For $M_{bol} = -4$, this formula gives $\dot{M} \sim 6\ 10^{-8} M_\odot$/yr. If one assumes that this result, derived in the solar neighbourhood, can still be applied to bulge stars with the same luminosity, it yields a gas-to-dust ratio in the range $\sim$100-500, depending on the dust properties. However, the gas-to-dust ratio should be significantly smaller at the base than at the tip of the "intermediate-AGB sequence" of Figure 6.

The nature of the dust of bulge stars with weak mass-loss will be discussed in a forthcoming paper (Blommaert et al. in preparation) from the ISOCAM-CVF spectral observation (5-16.5 μm) of a few $3' \times 3'$ ISOCAM fields in the bulge.

Let us stress that the intermediate AGB stars in the central Galactic bulge with low mass-loss rates (several 10^{-9} to close to 10^{-7} $M_\odot$/yr) seem rather similar in their properties to Solar Neighbourhood IRAS AGB stars with typical [12]-[25] colours in the range 0.2-1 (Guglielmo 1993, unpublished PhD thesis, Hacking et al. 1985).

6. Luminous Bulge AGB Stars

The apparently brightest stars detected by ISO at mid-infrared wavelengths form a loose group of $\sim$ 30 sources (see Figure 7) taking into account those saturated in DENIS bands, in the various magnitude-colour diagrams. They are brighter than the tip of the sequence of "intermediate-AGB" sources, which we have shown are AGB stars with low mass-loss rates. These stars have [15]$\lesssim$ 6, [7]$\lesssim$ 7, and $K_s \lesssim$ 8 in the various figures. Note that with conversion between K_s and M_{bol} (Table 3), this limit corresponds to $M_{bol} \lesssim$ -4.

A large proportion ($\sim$2/3) have at least two very red colours among K_s-[15]>2.0, [7]-[15]>1.2, K_s-[7]>1.0 and J-K_s >2.8, characteristic of larger mass-loss than for the intermediate-AGB sequence. It is tempting to identify them with the onset of the AGB "large mass loss" at $\dot{M}$$\sim$$10^{-7}$ $M_\odot$/yr. It is known that such a strong wind is classically associated with long period variability (LPV, see, e.g. Habing 1996 and references therein). From the SIMBAD data base, we have found two LPV stars previously identified in this field, IRAS17382-2830 and Terzan V3126 (Terzan & Gosset 1991). IRAS17382-2830 is an OH/IR star with $S_{25\mu m}/S_{12\mu m}$ = 2.12. It is denoted by "I" in Figure 7. Remarkably, this source (together with two other very bright 15μm sources) is not detected in our 1996 DENIS observations. Its derived colours are extremely red: K_s-[7]>7, K_s-[15]>9. Such very red colours are confirmed by the 1998 DENIS observations (see Table 1) where the source is detected, giving K_s = 11.7,

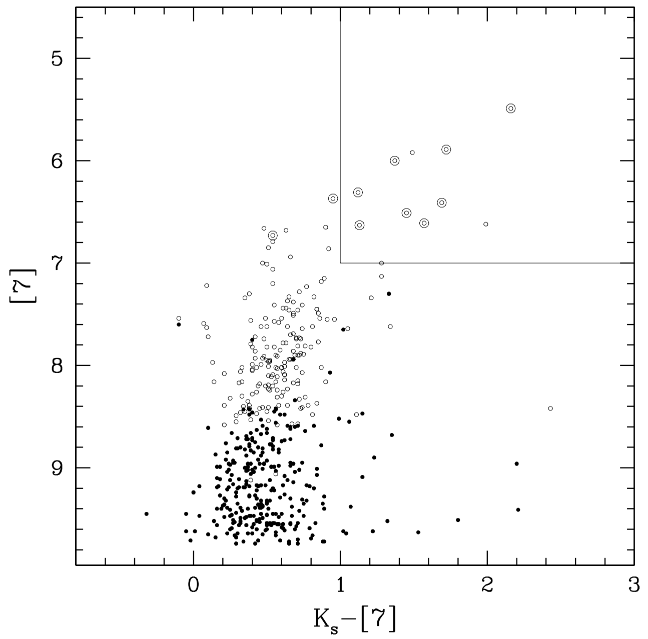

Fig. 9. [7]/K$_s$-[7] magnitude-colour diagram of all LW3 sources with unsaturated DENIS counterparts. Filled circles represent sources without a detection at LW3. Suspected variables are indicated additionally by large open circles. The region of high mass loss AGB is demarcated by the boxed region.

K$_s$-[7]=7.56 and K$_s$-[15]=9.43 (Schultheis et al, in preparation). These extreme near-IR colours are consistent with its very cold 12/25μm IRAS colour (see, e.g., Blommaert et al. 1998).

In order to investigate variability in this field we compared the observations performed with 6$''$ pixels, at two different dates (see Table 1) with both LW2 and LW3 filters. We consider that a bright source is a candidate to be considered for variability, when there is a 3σ difference in one band, or consistent weaker indications in both bands. The sources selected in this way are displayed with special symbols in Figures 4 to 9. We emphasise that this is just a positive indication in favor of variability, but without any rigorous statistical meaning. In particular, the significance of the candidate variables on the intermediate AGB sequence (Figure 6) is unclear, since they are not confirmed by variability in DENIS data (Schultheis et al. in preparation), and it is known that there is no strong variables on this sequence in Baade's Window (Glass et al 1999). On the other hand, with observations at only three epochs, we can miss a few variables. This is the case for example for the known variable Terzan V 3126.

A first striking feature in the distribution of these suspected variables is their high proportion in the regions of the magnitude-colour diagrams corresponding to the high mass-loss AGB stars defined above ($\dot{M}\gtrsim10^{-7}M_\odot$/yr) and delimited in Figures 4, 5, 6, 7 and 9. In all cases these candidate variables are at least 50% of the stars found there. Their proportion exceeds 80% in Figure 9 ([7]<7.0, [7]-[15] > 1.0. This region of the [7] *vs* [7] − [15] plane has been shown from analysis of ISOGAL data by Glass et al. (1999) to be best correlated with the LPV phenomenon in Baade Window fields. This identification of luminous variable stars using ISO photometry has been confirmed by preliminary comparisons of DENIS data at two epochs (Schultheis et al, in preparation), in particular for most individual stars of this field. Altogether, we have 16 candidate LPVs among the 33 brightest stars ([7] < 7.0).

Most of the sources with [7] < 7 which are not candidate LPVs are grouped in the region 6.4 < [7] < 7, 0.4 < K$_s$ - [7] < 1. Out of 12 sources there, only two are candidate variables. Of course, we have not enough data to claim with any certainty that any given star among the 10 other is not a variable. However, it is clear, from comparison with the similar group with K$_s$ - [7] > 1 where almost all stars are candidate variables, that the majority of these 10 stars are not strong variables. The relationship of this apparently non-variable group with AGB stars of similar K magnitude which are LPVs, and the relationship with less bright AGBs with however similar colours is still unclear (see also Glass et al 1999). It will be interesting to check in particular whether the difference between variable and non variable AGB stars in apparently similar evolutionary states is related to differences in metallicity or initial mass, or to a difference in mass loss history on the AGB. Another possibility is that most of the "non variable" bright stars are in the inner disk with $D < 8$ *kpc*, since their values of J-K$_s$ are smaller than the average value (curve C in Figure 4) for most of them.

7. Conclusion

ISOGAL, combining ISOCAM and DENIS data, is providing the first detailed and systematic mid-infrared study of an inner bulge field with sufficient sensitivity to isolate the entire AGB population. The ISOGAL performance allows a breakthrough in the analysis of infrared stellar populations, with an improvement of two orders of magnitude with respect to IRAS. The density of detected sources is close to the confusion limit with 3$''$ pixels at 7 μm. As expected, most of the sources are M giants of the bulge or central disk. In the low reddening fields analysed to date practically all bulge giants have near-infrared DENIS counterparts. This high proportion of associations is possible only because of the very good DENIS astrometry and the relatively good astrometry with ISOCAM. Sources detected above our completeness limit at 15 μm are mainly just above the RGB tip; they are thus mostly AGB stars. Sources detected only at 7 μm are mainly normal bulge red giants just below the RGB tip.

The completeness and reliability of detection at 7 μm and 15 μm of point sources are high and well quantified down to $\sim$ 15 mJy and $\sim$ 10 mJy respectively. The photometric accuracy is reduced by a variety of effects:

by the complex time- and illumination history-dependant behaviour of ISOCAM pixels, especially in regions with a very high density of bright sources, and also by the integration time available for a wide-area survey. However, the photometric accuracy we have achieved is good enough to be able to take advantage of the rich information provided by the combination of the five wavelength data of ISOGAL+DENIS. Of particular importance is our ability to detect reliably quite small reddening-corrected 15 μm excesses. A detailed analysis of the stellar populations is also much eased by the overwhelming preponderance of bulge or central disk stars with a well defined distance, and, in the present field, by the relatively low and constant interstellar reddening in front of the whole field studied. We have shown here that our ISOGAL survey is ideal (though not unique) for analysis of AGB stars with large mass-loss rates ($\dot{M} \geq 10^{-7} M_\odot$/yr), by providing a complete census in the field, independent of large amplitude variability.

The most important conclusion for future analyses from the present analysis is our demonstration that the combination of near-IR (DENIS) and mid-IR (7 μm and 15 μm) ISOGAL data allows reliable detection of circumstellar dust and low rates of mass-loss in bulge AGB stars not deducible from near-infrared data alone. ISOGAL is uniquely suitable for systematic studies of AGB stars with low rates of mass-loss in the whole inner Galaxy, especially in the bulge. The very small amounts of dust associated with low rates of mass loss are undetectable in the near-infrared, both in absorption and in emission, while being readily detectable at 15 μm. Stars with low rates of mass loss are too faint to have been detectable by IRAS, except in the solar neighbourhood; most of them will escape detection by MSX because of the confusion limit arising from the 18$''$ MSX pixels, which have areas almost an order of magnitude larger than those used for ISOGAL. Although mid-infrared evidence for dust emission corresponding to low rates of mass loss is seen in the IRAS data for AGB stars in the solar neighbourhood, inevitable distance uncertainties make the analysis of such IRAS data for mass-loss rates and AGB evolution much less clear-cut.

The most important immediate scientific conclusion of this paper is our detection of low rates of mass loss which are ubiquitous for red giants with luminosities just above or possibly close to the RGB tip, and thus still in relatively early stages. The most luminous of these stars, that we defined as "intermediate" AGB (in the early AGB thermal pulse phase), form a well defined sequence in the [15]/K$_s$-[15] and [15]/[7]-[15] magnitude-colour planes. In order to explain the colours the presence of dust is required, with (model-dependant) dust mass-loss rates of a few 10^{-11} $M_\odot$/yr. It is thus well established that dust formation is already associated with weak mass-loss during the early TP-AGB phase, This obviously puts important constraints on the physics of dust formation.

These first results can obviously be improved and exploited in several ways. For the data presented for this specific field, we still hope to improve the photometry and the reliability of the ISOGAL data, in particular by including the verification observations not yet fully exploited. The study of mass-losing red giants will be extended to the other 200 ISOGAL fields : i) in a straightforward way to the other ISOGAL bulge fields with $|b| > 1^0$, as already done for the ISOGAL observations of two Baade Window fields (Glass et al. 1999); ii) to the bulk of the ISOGAL fields closer to the Galactic plane, where there is large and variable extinction, and where the uncertainty on the distance and the mixing with young stars somewhat complicate the analysis. We are currently analysing the surface density of the various classes of AGB stars to characterize the structure and stellar populations of the bulge, to determine to what extent it is meaningful to consider the various structures: bulge, central disk, bar, central cluster, and so on.

As concerns the theoretical interpretation, much work is still needed in order to:

i) Improve the models of red giants with weak mass-loss both for photospheric and for dust emission. Many questions can be addressed: what is the chemical nature of the dust, considering silicates and possible other components; is the base of the large spread we have observed in I-J colours at fixed luminosity a metallicity effect; and more generally, how can we disentangle the effects due to initial mass, age and metallicity?

ii) Use our ISOGAL results to further constrain the models of dust formation and of TP-AGB evolution, and in particular: determine whether dust formation can begin in RGB stars close to the RGB tip, or whether it is specific of AGB stars; and explain dust formation in the context of very weak mass-loss.

Acknowledgements
This work was carried out in the context of EARA, the European Association for Research in Astronomy. We would like to thank M. Pérault, P. Hennebelle, S. Ott, R. Gastaud, H. Aussel, and F. Viallefond for useful discussions during the course of the reduction of the ISO data. We thank the referees, especially, J.A. Frogel, for their very constructive and useful suggestions. SG was supported by a fellowship from the Ministere des Affaires Etrangères, France. MS acknowledges the receipt of an ESA fellowship. The DENIS project is partially funded by European Commission through SCIENCE and Human Capital and Mobility plan grants. It is also supported, in France by the Institut National des Sciences de l'Univers, the Education Ministry and the Centre National de la Recherche Scientifique, in Germany by the State of Baden-Würtemberg, in Spain by the DG1CYT, in Italy by the Consiglio Nazionale delle Ricerche, in Austria by the Fonds zur Förderung der wissenschaftlichen Forschung und Bundesministerium für Wissenshaft und Forschung, in Brazil by the Foundation for the development of Scientific Research of the State of Sao Paulo (FAPESP), and in Hungary by an OTKA grant and an ESOC&EE grant.

Appendix A: Definition of ISOGAL Fluxes and Magnitudes

The fluxes and magnitudes used were defined in the following way (Blommaert 1998). The ISOCAM units of ADU/gain/sec were first converted into mJy/pixel units within CIA, with the conversion factors:

$$F(mJy) = (ADU/G/s)/2.33 \tag{A1}$$

for LW2 and

$$F(mJy) = (ADU/G/s)/1.97 \tag{A2}$$

for LW3. These are correct for a $F_\lambda \sim \lambda^{-1}$ power spectrum at wavelengths 6.7 μm and 14.3 μm respectively.

Magnitudes are defined by

$$mag(LW2) = [7] = 12.39 - 2.5 \times log[F_{LW2}(mJy)] \tag{A3}$$

$$mag(LW3) = [15] = 10.74 - 2.5 \times log[F_{LW3}(mJy)] \tag{A4}$$

where the zero point has been chosen to provide zero magnitude for a Vega model flux (A0V star, not including the infrared excess emission of the circumstellar disk) at the respective wavelengths mentioned earlier.

Appendix B: Details of Data Reduction and Quality; Cross-Identifications

B.1. ISOGAL

The special procedure for ISOGAL source extraction, developed by Alard et al (in preparation), uses several "CIA" [4] procedures not yet implemented in the standard (auto-analysis) treatment (corrections for distortion of the ISOCAM field, and for time behaviour ["vision" and " inversion" methods]). It also includes a sophisticated source extraction, after a regularisation of the point-spread-function (PSF). Indeed, there is not yet a good standard procedure to fully correct for the time behaviour effects for fields such as ISOGAL ones with strong sources and background. Here we have used the fluxes given by the "inversion" method, which provides better photometry, but we have used the "vision" method to identify and drop the false sources generated by the detector "memory" of bright sources previously observed at a different location on the sky, but in the same pixel.

After the elimination of the false replication sources, the source counts in this field are 599 and 282 respectively in LW2 ([7] < 9.75) and LW3 ([15] < 8.5) . This is indeed close to the confusion limit for LW2 sources (85 pixels [$3'' \times 3''$] per source, density 1.7 10^4 deg^{-2}), but farther from this limit for LW3 ones (8.1 10^3 deg^{-2}).

[4] "CIA" is a joint development by the ESA Astrophysics Division and the ISOCAM Consortium.

B.2. DENIS

For DENIS sources, the sensitivity is mostly limited by confusion in the K_s and J bands ($\sim 7.7 \times 10^4$ deg^{-2} [for $K_s < 12$ and $J < 14$], giving $\sim$19 pixels ($3'' \times 3''$) per source). The completeness limit is thus probably close to 11.5 in the K_s band and 13.5 in the J band. The density at the sensitivity limit in the I band, ~ 18 , is farther from confusion (density ~ 1.3 $10^5 deg^{-2}$ with $1'' \times 1''$ pixels).

Independent magnitudes are available for many DENIS sources in the overlap region between adjacent observations. Analysis of these repeated observations shows that the internal dispersion in the photometry, in this crowded region, is less than 0.1 mag for $K_s < 11$, $J < 13.5$ and $I < 16.5$ (it rises to 0.18 mag for $K_s < 13$, 0.13 mag for $J < 14.5$ and 0.2 for $I < 17.5$). For the determination of the zero point all standard stars observed in this night have been used. We derived the following zero points: I = 23.45, J = 21.59 and K_s = 19.85, respectively. The internal rms in the zero-points is found to be 0.03, 0.07 and 0.04 mag in the K_s, J and I bands respectively.

B.3. Cross-Identifications

We have now routine standard procedures for ISOGAL-ISOGAL and DENIS-ISOGAL cross-identifications (Copet et al. in preparation). The good quality of the pointing of ISO and of the correction of the ISOCAM field distortions permits, after optimisation of a small rotation-translation of the fields, a reduction of the rms of the nominal offsets of matched sources to $\sim 0.6''$ and $\sim 1.1''$ for LW3/LW2 and ISOGAL/DENIS respectively. However, the search radius was fixed at a large value, $2.7''$, for LW3/LW2 associations in order not to miss associations. The chance of spurious association with an LW2 source is then $\sim$ 4%. Because of the very high density of DENIS sources, the search radius was reduced to $2.1''$ for the DENIS/ISOGAL associations. Nevertheless, the density of the DENIS sources is so high that the chance of spurious associations remains $\sim$ 10% for K_s sources with $K_s < 12$. The chance of spurious association is reduced to 5% when one limits the associations to $K_s = 11$. A substantial fraction of the ISO sources have thus been identified with DENIS sources. Out of a total number of 599 LW2 sources, 557 (93%) are matched with a $K_s < 12$ source, 552 with a JK_s source and 522 with an IJK_s source. Out of 282 LW3 sources, 248 (86%) are matched with an LW2 source, 237 (84%) with a JK_s/LW2, and 221 (78%) with an IJK_s/LW2 source. The number of LW2/LW3 sources without K_s or LW3/K_s sources without LW2 is very small, 10 in both cases .

B.4. ISOGAL Completeness and Photometry

In order to check the completeness of LW3 sources, we can use the more sensitive LW2 observations. One can check, for instance, that only 13 LW2 sources with [7] $<$ 8.3, among 183 in total, are missing in LW3. From the known range of values of [7] - [15], we can conclude from Figure 1 that the completeness of LW3 sources is close to 100% for [15] $<$ 7.5 ($\sim$ 20 mJy) and $\sim 65-90\%$ in the range 7.5 $<$ [15] $<$ 8.5 ($\sim 8-20$ mJy).

DENIS K_s detections can be used in a similar way to estimate the completeness of LW2 sources. Figure 1 compares the number of LW2 sources detected per half magnitude bin with an approximate estimate of the number expected from K_s sources with typical colours. It is seen that the detections are practically complete for [7] $<$ 8.5 ($\sim$ 35 mJy) and that they remain more than 80% complete for 8.5 $<$ [7] $<$ 9.5 ($\sim 15-35$ mJy); however, the completeness rapidly decreases below $\sim$ 15 mJy. This incompleteness is mainly due to confusion.

The quality of ISOGAL photometry has been checked in this field (Table 1) and others by repeated observations both with $6''$ pixels (Ganesh et al. in preparation). The uncertainty thus proved to be better than $\sim$ 0.2 mag rms above $\sim$ 15 mJy in both bands. It is poorer for weaker sources, especially in the LW3 band. One can expect a similar repeatibility accuracy with $3''$ pixels. However, this does not take into account systematic errors. In particular, the comparison of the $3''$ and $6''$ pixels measurements which were performed on this field shows a small systematic difference in the fluxes, with average differences up to 0.1-0.2 mag rms. Further work is in progress to understand these details, but the effect may be explained by the source confusion as is discussed in DePoy et al (1993). Our photometry is thus still uncertain by a few tenths of a magnitude systematically.

The photometry is expected to be poorer on the edges of the ISOGAL image: in such a small raster (4×7 pointings), $\sim$ 40% the image is observed with a single exposure instead of the double exposure on average for the points of the central part. In addition, the source extraction is not able to recover the full intensity of sources very close to the edges within a few pixels.

References

Bertelli, G., et al., 1994 A&AS, 106, 275

Binney, J.J., Gerhard, O.E., and Spergel D.N., 1997, MNRAS, 288, 365

Blommaert, J.A.D.L, 1998: ISOCAM Photometry Report, http://www.iso.vilspa.esa.es/users/expl_lib/CAM_list.html

Blommaert, J.A.D.L., van der Ween, W.E.C.J., van Langevelde, H.J., Habing, H.J., Sjouwerman, L.O., 1998, A&A 329, 991

Cesarsky, C., et al. 1996 A&A, 315L, 32

Cutri, R. M. 1998, BAAS, 30, No. 2,#64.02.

Depoy, D.L., Terndrup, D.M., Frogel, J.A., Atwood, B., Blum, R., 1993,AJ 105,2121

Egan, M.P., Shipman, R.F., Price, S.D., Carey, S.J., Clark, F.O., Cohen, M., 1998, ApJ 494, 199

Epchtein N., et al., 1997, Messenger 87, 27

Frogel, J.A., Whitford, A.E., 1987, ApJ 320, 199 (FW)

Frogel, J.A., Terndrup, D.M., Blanco, V.M., Whitford, A.E., 1990, ApJ 353, 494

Frogel, J.A., Tiede, G.P., Kuchinski, L.E., 1999, AJ in press (astro-ph/9901328)

Glass, I.S., Whitelock, P.A., Catchpole, R.M., Feast, M.W., 1995, MNRAS 273, 383

Glass, I.S., Ganesh, S., Alard, C., Blommaert, J.A.D.L., Gilmore, G., Lloyd Evans, T., Omont, A., Schultheis, S., Simon, G., 1999, MNRAS in press (astro-ph/9904010)

Groenewegen, M.A.T., 1997, in "The Impact of Large Scale Near-IR Sky Surveys", F. Garzon et al. (eds). Kluwer. Page 165

Guglielmo, F., 1993, Thesis, Universite Paris VII

Habing, H.J., 1996, Astron. Astrophys. Rev. 7, 97

Hacking, P., et al., 1985, PASP 97, 616

Le Bertre, T., Lebre, A., Waelkens, C. 1999, eds, Proceedings of IAU Symposium 191

Omont A. & The ISOGAL Collaboration 1999, in "Astrophysics with Infrared Surveys: A Prelude to SIRTF", Pasadena, ASP Conference Series, in press

Omont A. et al. 1999b, to appear in 'The Universe as seen by ISO', eds. P. Cox and M.F. Kessler, ESA Special Publications series (SP-427)

Pérault M., Omont A., Simon G., Séguin P., Ojha D., Blommaert J., Felli M., Gilmore G., Guglielmo F., Habing H., Price S., Robin A., de Batz B., Cesarsky C., Elbaz D., Epchtein N., Fouqué P., Guest S., Levine D., Pollock A., Prusti T., Siebenmorgen R., Testi L., Tiphène D., 1996, A&A 315, L165

Persson, S.E., Murphy, D.C., Krzeminski, W., Roth, M., Rieke, M.J., 1998, AJ 116, 2475

Price, S.D., Tedesco, E.F., Cohen, M., Walker, R.G., Henry, R.C., Moshir, M., Paxton, L.J., Witterborn, F.C., 1997, IAU Symp. 179, p115

Reimers, D., 1975, in "Problems in Stellar Atmospheres and Envelopes" B. Baschek , W.H. Kegel, G. Traving (eds), Springer, Berlin, p 229

Skrutskie, M.F. et al. 1997, in "The Impact of Large Scale Near-IR Sky Surveys," p187-195, F. Garzon et al. (eds.), Kluwer (Netherlands).

Terzan, A. , Gosset E., 1991, A&AS 90, 451

Tiede, G.P., Frogel, J.A., Terndrup, D.M., 1996, AJ 110, 2788

Unavane, M., Gilmore, G., Epchtein, N., Simon, G., Tiphene, D., de Batz, B., 1998, MNRAS 295, 119

van der Veen, W.E.C.J., Habing, H.J., 1990, A&A 231, 404